

Xenic Acid: Reduction at the Dropping-Mercury Electrode

Abstract. Xenic acid is reduced at the dropping-mercury electrode in a single step to xenon. The half-wave potential for the reduction of xenic acid changes from approximately -0.10 to -0.360 volt against a saturated $\text{Hg}_2\text{SO}_4\text{-Hg}$ reference electrode in the pH range 4.60 to 8.00. The diffusion current varies linearly with concentration of xenic acid.

Investigation of xenic acid reduction at the dropping mercury electrode was initiated with the hope of establishing whether xenic acid is reduced in steps with the formation of stable intermediate species of lower oxidation states or whether it is reduced directly to atomic xenon.

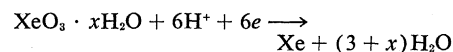
Aqueous solutions of xenic acid, $\text{XeO}_3 \cdot x\text{H}_2\text{O}$, may be obtained by the hydrolysis either of xenon tetrafluoride, XeF_4 , or xenon hexafluoride, XeF_6 , as has been described by Dudley *et al.* (1) and Williamson and Koch (2). Xenic acid is a very weak acid, comparable to orthotelluric acid, H_6TeO_6 , and has an oxidation potential which is possibly as negative as periodic acid.

A Sargent model XXI recording polarograph and an H-polarographic cell equipped with a thermostat were used for the polarographic study. Buffered or unbuffered 0.1M potassium sulfate solution was used as the supporting electrolyte and the concentration of the xenic acid was adjusted in the range 4×10^{-5} to $2.0 \times 10^{-4}M$. Nitrogen, purified by passing it over hot copper turnings, was bubbled through the solutions to deaerate them.

This process was carried out in the absence of mercury to prevent the reduction of the xenic acid, and a polarogram was made immediately. A typical polarogram of xenic acid in the potassium sulfate electrolyte is shown in

Fig. 1, and the results are summarized in Table 1.

In the potassium sulfate electrolyte, xenic acid forms a well-defined cathodic wave. This wave is preceded by a very small anodic wave which eventually coalesces with the cathodic wave as the concentration of xenic acid increases. Well-defined anodic waves preceding the reduction of periodate and of orthotellurate have been reported by Jensovsky (3), and Jaselskis and Lanese (4), respectively. Thus it appears that xenic acid, in the first step, oxidizes mercury and forms an unstable and slightly soluble mercurous xenate. The cathodic wave corresponds to a six electron reduction process. The number of electrons taking part in the reduction process has been calculated by comparing the periodate reduction to iodic acid at pH 6.4. For the same concentration, the reduction wave for xenic acid is three times greater than that of periodate, which has been established to be a two electron reduction. The half-wave potential $E_{1/2}$, becomes more negative with increasing pH, as would be expected for the reduction reaction



For a reversible process the change of pH by one unit should produce a shift of the half-wave potential by 0.06 volt. However, this is not the case, as shown in Table 1, indicating that the reduction process is irreversible.

The cathodic current is proportional to the square root of the mercury head and changes approximately by 2 percent per degree Celsius indicating that the reduction process is primarily diffusion controlled.

That the cathodic wave is directly proportional to the concentration of xenic acid present, in the range 4×10^{-5} to $2 \times 10^{-4}M$ is supported by the constancy of $i/Cm^{2/3}t^{1/6}$, where

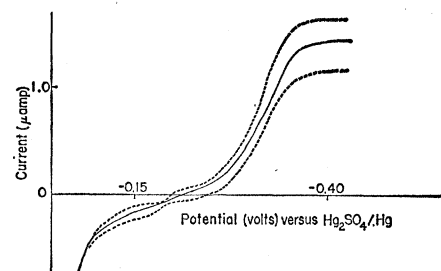


Fig. 1. Polarogram of $8.24 \times 10^{-5}M$ xenic acid in 0.1M potassium sulfate. Dashed lines, maximum and minimum current; solid line, average current.

i is the diffusion current, C is the concentration of xenic acid, m is the mass flow of mercury in milligrams per second, and t is the drop time in seconds.

BRUNO JASELSKIS

Department of Chemistry, Loyola University, Chicago, Illinois

References and Notes

1. F. Dudley, G. Gard, G. Cady, *Inorg. Chem.* **2**, 228 (1963).
2. S. M. Williamson and C. W. Koch, *Science* **139**, 1046 (1963).
3. L. Jensovsky, *Collection Czech. Chem. Commun.* **22**, 311 (1957).
4. B. Jaselskis and J. G. Lanese, *J. Inorg. Nucl. Chem.* **24**, 399 (1962).
5. I thank Messrs. Malm and Appelman from the Argonne National Laboratories for the sample of xenic acid.

9 January 1964

Hydrogen Energy Levels: Perturbation Caused by Proton Structure

Abstract. The shifts in the lowest electronic energy levels of the hydrogen atom caused by the extended charge distribution of the proton have been calculated and found to be of the order of the unexplained portion of the Lamb shift for these levels.

The analysis of high-energy electron scattering from hydrogen has shown that the proton is not a point charge (1). Satisfactory agreement with the experimental data is obtained by representing the proton as a spherically symmetric cloud of charge whose density is an exponentially decreasing function of the radial distance from its center and whose radius (root mean square) is approximately 0.80×10^{-13} cm. Such a charge-density distribution, suitably normalized, is given by the equation

$$\rho(r) = (e\alpha^3/8\pi) \exp(-\alpha r) \quad (1)$$

where ρ is the charge density, r is the radial coordinate, e is the electronic charge, and $\alpha = 4.32 \times 10^{13} \text{ cm}^{-1}$.

Table 1. Polarographic characteristics of xenic acid.

Conc. of xenic acid ($M \times 10^5$)	pH of supporting electrolyte	$E_{1/2}$ volt against $\text{Hg}_2\text{SO}_4\text{-Hg}$	Diffusion current (μamp)	$i/Cm^{2/3}t^{1/6} \times 10^4$
4.12	6.4*	-0.29	0.62	0.993
8.24	6.4*	-0.32	1.38	1.105
12.36	6.4*	-0.32	2.04	1.090
16.48	6.4*	-0.32	2.70	1.082
20.60	6.4*	-0.32	3.35	1.074
8.24	4.6†	-0.10	1.30	1.042
8.24	5.3‡	-0.24	1.36	1.090
8.24	8.0‡	-0.36	1.40	1.021

* Unbuffered 0.10M potassium sulfate solution used as the supporting electrolyte. † Supporting electrolyte of 0.1M potassium sulfate and 0.02M acetic acid, with the pH adjusted by the addition of KOH. ‡ Supporting electrolyte of 0.1M potassium sulfate and 0.2M NaH_2PO_4 with the pH adjusted by the addition of KOH.

The electrostatic potential within which the electron moves will differ from the usual Coulomb form it would assume if the proton were strictly a point charge. The actual potential energy may be calculated for a known proton charge-density distribution from the relation

$$V(r) = -(4\pi e/r) \int_0^r \rho(r') r'^2 dr' - (4\pi e) \int_r^\infty \rho(r') r' dr' \quad (2)$$

where $V(r)$ is the potential energy and the other symbols have the same meaning as before. If the integrals in Eq. 2 are evaluated with the proton density distribution of Eq. 1, the result is

$$V(r) = -e^2/r + (e^2/r) [1 + (\alpha r/2)] \exp(-\alpha r) \quad (3)$$

Therefore, the electrostatic potential energy consists of the usual attractive Coulomb term plus the short-ranged term $V'(r)$ where

$$V'(r) = (e^2/r) [1 + (\alpha r/2)] \exp(-\alpha r) \quad (4)$$

As a result of this additional term, the electronic energy levels will be shifted from the values for hydrogen by an amount given, to a first approximation, by $V'_{nlm, nlm}$, the expectation value of $V'(r)$ in the state whose quantum numbers are n , l , and m (2). Calculation of this expectation value for the $1s$ and $2s$ states gives

$$V'_{100, 100} = (1.52 \times 10^{-10}) e^2/a_0$$

$$V'_{200, 200} = (0.19 \times 10^{-10}) e^2/a_0$$

where $a_0 = 0.53 \times 10^{-8}$ cm is the Bohr radius. Since the energy of the state of principal quantum number n is given by

$$E_n = -e^2/(2n^2 a_0)$$

these shifts represent approximately 3.0 and 1.5 parts in 10^{10} of the corresponding unperturbed energy values. The term $V'(r)$ also causes a splitting of the $2s$ and $2p$ energy levels which is of the same order of magnitude as $V'_{200, 200}$ and which corresponds to a frequency of approximately 0.10 megacycle. It is of interest to note that this frequency is of the same order of magnitude as the still-unexplained difference between the measured and the field theoretical values of the Lamb shift for these levels (3).

Calculations with charge density distributions other than the exponential form of Eq. 1 lead to comparable values of the aforementioned effects.

WILLIAM S. PORTER

Department of Physics, Bucknell University, Lewisburg, Pennsylvania

20 MARCH 1964

References

1. R. Hofstadter, *Ann. Rev. Nucl. Sci.* **7**, 231 (1957).
2. R. H. Dicke and J. P. Wittke, *Introduction to Quantum Mechanics* (Addison-Wesley, Reading, Mass., 1960), pp. 226-258.
3. A. J. Layzer, *Phys. Rev. Letters* **4**, 580 (1960).
- 4 December 1963

Simultaneous Studies of Firing Patterns in Several Neurons

Abstract. *A tungsten microelectrode with several small holes burnt in the vinyl insulation enables the action potentials from several adjacent neurons to be observed simultaneously. A digital computer is used to separate the contributions of each neuron by examining and classifying the waveforms of the action potentials. These methods allow studies to be made of interactions between neurons that lie close together.*

The extent to which physically contiguous neurons form domains or functional aggregates is a fundamental problem in studying the organization of the central nervous system. That such domains exist in sensory cortical regions has been shown by electrophysiological methods: a "cylinder," measuring 200 μ in diameter and running through the depths of the cortex, forms some sort of functional unit in the processing of sensory information (1, 2). Elaboration of neural interactions within such a functional aggregate has proved difficult. A macroelectrode picks up the summated (slow) activity of thousands to millions of neurons while a microelectrode usually picks up the electrical activity of one cell at a time. It is obviously necessary to bridge these extremes by recording simultaneously and separably the electrical activity of small clusters of neurons.

Some data on the simultaneous activity of two neurons have been obtained from microelectrode recordings which show two spike trains that are distinguishable because of widely different amplitude (2, 3). Other authors have used several microelectrodes independently inserted into the structure being studied (4). With this technique it is difficult to ensure that the neurons under study are closely spaced because of deformation of the tissues and flexibility of the microelectrodes. In addition, the neurons are more likely to be damaged as the number of microelectrodes is in-

creased. Changes in neuron connectivity, pressure changes, and alterations in microcirculation are not easily controlled or evaluated by the experimenter. Accordingly, we approached the problem by developing a single microelectrode that would allow three to five different trains of action potentials to be recorded simultaneously. Since the geometry relative to the electrode differs for each neuron under observation, the various action potentials may be distinguished by their waveform.

While working with very large (30 to 50 μ) tungsten microelectrodes we frequently observed the activities of a number of neurons, unfortunately with very low amplitudes because of the large open area of the electrode. Tungsten microelectrodes with a smaller open area (5 to 10 μ) produce excellent action-potential amplitudes, but allow only one or two neurons to be observed simultaneously. Obviously, we required an electrode with a total open area comparable to the usual 5- to 10- μ electrode, but with this open area distributed over some 100 μ of the shaft.

Such a "distributed area" microelectrode can be produced from the usual 10- μ tungsten microelectrode (5) by damaging the vinyl insulation. Under 100-power magnification, the tip of the electrode is inserted into a hanging drop of clean mineral oil for protection. Another microelectrode is brought up at right angles to within 5 to 10 μ of the shaft some 50 μ from the tip, and a short series of sparks from a Tesla coil (6) is applied between the two electrodes. The intensity and duration of the sparks must be determined experimentally. By this procedure several small holes are burned in the vinyl insulation at random points along the first 100 μ of the microelectrode shaft. When tested, the electrode shows bubbling at these several points as well as at the tip. By proper design of the various electrode holders and saline test bath, the entire test-spark-test procedure for an electrode can be carried out under a microscope in a few minutes.

Typical action potential data observed with the distributed area tungsten microelectrode are shown in Fig. 1A. This example is taken from the dorsal cochlear nucleus of a cat anesthetized with Nembutal; similar results have been obtained in various brain-stem, cerebellar, and cortical lo-